RESEARCH ARTICLE OPEN ACCESS

Electroelastic Response of a Piezoelectric Semi-infinite Body with D_∞ Symmetry to Surface Friction

Masayuki Ishihara*, Yoshihiro Ootao**, and Yoshitaka Kameo***
*(Graduate School of Engineering, Osaka Prefecture University;)
**(Graduate School of Engineering, Osaka Prefecture University;)
***(Institute for Frontier Medical Sciences, Kyoto University;)

ABSTRACT
In this paper, with the aim of developing a nondestructive evaluation technique using piezoelectric signals in wooden materials, we theoretically study the electroelastic field in a semi-infinite body with D_∞ symmetry subjected to surface friction parallel to the ∞-fold rotation axis. By applying the analytical technique previously proposed by us, we formulate expressions for electroelastic field quantities, including electric potential, electric field, electric displacement, elastic displacement, strain, and stress by using two "elastic displacement potential functions" and two "piezoelastic displacement potential functions." These potential functions and, consequently, the electroelastic field quantities are formulated using Fourier transforms in order to satisfy electroelastic boundary conditions. We carried out numerical calculations to correctly evaluate field quantities inside the body and at its surface. As a result, we were successful in quantitatively elucidating the surface electric displacement in response to the elastic stimulus of surface friction and suggested the possibility of a nondestructive evaluation technique using piezoelectric signals.
***Keywords* -** D_∞ symmetry, electroelastic problem, piezoelectric body, theoretical analysis

I. Introduction

Because of rising demands to reduce the global carbon footprint, wooden materials have attracted considerable attention in engineering production as "carbon-neutral" materials. To ensure wooden materials of satisfactory quality, nondestructive evaluation techniques need to be developed. The electroelastic behaviors of wood, which is known as a piezoelectric material [1], have been investigated using piezoelectric effects. Piezoelectric signals were related to the profiles of defects [2-4], deformation [5, 6], and the stress–strain relation [7, 8].

Because wooden materials contain complicated microstructures, their detailed electroelastic behavior needs to be investigated from a microscopic standpoint. Such an approach, however, entails a considerably high computational cost and is impractical for engineering applications. Therefore, a macroscopic approach is required. From a macroscopic viewpoint, woods are generally recognized as orthotropic materials with their principal axes in the longitudinal, radial, and tangential directions [9, 10].

Furthermore, according to another approach, woods are considered to have D_∞ symmetry [5-8]. This is the consequence of an aggregation of natural cellulose chains in a certain manner [1, 8]. D_∞ symmetry is characterized by an "∞-fold rotation axis" and a "two-fold rotation axis" perpendicular to it [11]. In other words, the material is isotropic within the plane perpendicular to the longitudinal direction. One of the most striking characteristics of a body with D_∞ symmetry is the coupling between the shear strain (or shear stress) in the plane parallel to the ∞-fold rotation axis and the electric field (or electric displacement) perpendicular to the plane.

Considering the importance of electroelastic problems in wooden materials, we developed an analytical technique to obtaining general solutions to coupled electroelastic problems in bodies with D_∞ symmetry, and presented new possibilities in the theoretical investigation of the electroelastic behavior of wooden materials [12]. In that study, by way of a trial application of the technique, we treated a semi-infinite body and investigated the response of "elastic quantities," such as stress and strain, resulting from "electric stimulus" by an electric potential on its surface. In order to develop nondestructive evaluation techniques, however, the response of electric quantities due to elastic stimuli need to be elucidated.

In this paper, therefore, we study the electroelastic field in a semi-infinite body subjected to surface friction parallel to the ∞-fold rotation axis in order to explore techniques of nondestructive evaluation. By applying the analytical technique previously proposed by us [12], electroelastic field quantities, including electric potential, electric field, electric displacement, elastic displacement, strain, and stress, can be expressed by two "elastic displacement potential functions" and two "piezoelastic displacement potential functions." These potential functions and, consequently, the electroelastic field quantities are formulated to satisfy electroelastic boundary conditions. Moreover, we performed numerical calculations to investigate the effects of the elastic stimulus modeled by the surface friction on the electric quantities.

II. Theoretical analysis

2.1 Problem

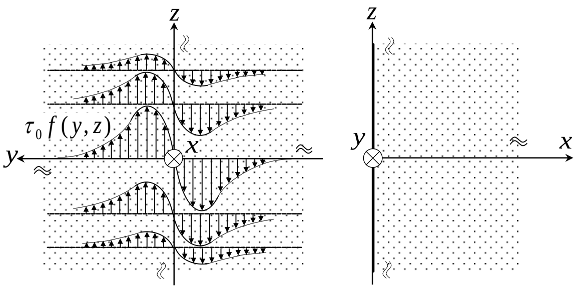

Fig. 1: Analytical model

We consider a semi-infinite piezoelectric body $(x>0)$ with D_∞ symmetry, as shown in Fig. 1, where the z-axis is parallel to the ∞-fold rotation axis of the body. The surface of the body is subjected to surface friction $\tau_0 f(y,z)$, which is anti-symmetric and symmetric with respect to y and z, respectively. The surface $x=0$ is chosen as the reference plane of electric potential. The displacements and electric potential are assumed to be zero at infinity. Our purpose in this section is to formulate the components of displacement, strain, stress, electric field, and electric displacement in the Cartesian coordinate system (x,y,z), which are denoted as (u_x,u_y,u_z), $(\varepsilon_{xx},\varepsilon_{yy},\varepsilon_{zz},\varepsilon_{yz},\varepsilon_{zx},\varepsilon_{xy})$, $(\sigma_{xx},\sigma_{yy},\sigma_{zz},\sigma_{yz},\sigma_{zx},\sigma_{xy})$, (E_x,E_y,E_z), and (D_x,D_y,D_z), respectively and to formulate the electric potential Φ.

2.2 Fundamental equations

The fundamental equations for the problem stated in Subsection 2.1 are provided by the displacement-strain relations

$$\left.\begin{aligned}&\varepsilon_{xx}=\frac{\partial u_x}{\partial x},\ \varepsilon_{yy}=\frac{\partial u_y}{\partial y},\ \varepsilon_{zz}=\frac{\partial u_z}{\partial z},\\&2\varepsilon_{yz}=\frac{\partial u_y}{\partial z}+\frac{\partial u_z}{\partial y},\ 2\varepsilon_{zx}=\frac{\partial u_z}{\partial x}+\frac{\partial u_x}{\partial z},\\&2\varepsilon_{xy}=\frac{\partial u_x}{\partial y}+\frac{\partial u_y}{\partial x}\end{aligned}\right\}, \tag{1}$$

the relation between the electric potential and electric field

$$E_x=-\frac{\partial\Phi}{\partial x},\quad E_y=-\frac{\partial\Phi}{\partial y},\quad E_z=-\frac{\partial\Phi}{\partial z}, \tag{2}$$

the constitutive equations

$$\left.\begin{aligned}&\begin{Bmatrix}\sigma_{xx}\\\sigma_{yy}\\\sigma_{zz}\\\sigma_{yz}\\\sigma_{zx}\\\sigma_{xy}\end{Bmatrix}=\begin{bmatrix}c_{11}&c_{12}&c_{13}&0&0&0\\&c_{11}&c_{13}&0&0&0\\&&c_{33}&0&0&0\\&&&c_{44}&0&0\\&&&&c_{44}&0\\\text{sym.}&&&&&\dfrac{c_{11}-c_{12}}{2}\end{bmatrix}\begin{Bmatrix}\varepsilon_{xx}\\\varepsilon_{yy}\\\varepsilon_{zz}\\2\varepsilon_{yz}\\2\varepsilon_{zx}\\2\varepsilon_{xy}\end{Bmatrix}\\&-\begin{bmatrix}0&0&0\\0&0&0\\0&0&0\\e_{14}&0&0\\0&-e_{14}&0\\0&0&0\end{bmatrix}\begin{Bmatrix}E_x\\E_y\\E_z\end{Bmatrix}\end{aligned}\right\}, \tag{3}$$

$$\left.\begin{aligned}&\begin{Bmatrix}D_x\\D_y\\D_z\end{Bmatrix}=\begin{bmatrix}0&0&0&e_{14}&0&0\\0&0&0&0&-e_{14}&0\\0&0&0&0&0&0\end{bmatrix}\begin{Bmatrix}\varepsilon_{xx}\\\varepsilon_{yy}\\\varepsilon_{zz}\\2\varepsilon_{yz}\\2\varepsilon_{zx}\\2\varepsilon_{xy}\end{Bmatrix}\\&+\begin{bmatrix}\eta_{11}&0&0\\&\eta_{11}&0\\\text{sym.}&&\eta_{33}\end{bmatrix}\begin{Bmatrix}E_x\\E_y\\E_z\end{Bmatrix}\end{aligned}\right\}, \tag{4}$$

the equilibrium equations of stresses

$$\left.\begin{aligned}&\frac{\partial\sigma_{xx}}{\partial x}+\frac{\partial\sigma_{xy}}{\partial y}+\frac{\partial\sigma_{zx}}{\partial z}=0,\\&\frac{\partial\sigma_{yy}}{\partial y}+\frac{\partial\sigma_{yz}}{\partial z}+\frac{\partial\sigma_{xy}}{\partial x}=0,\\&\frac{\partial\sigma_{zz}}{\partial z}+\frac{\partial\sigma_{zx}}{\partial x}+\frac{\partial\sigma_{yz}}{\partial y}=0\end{aligned}\right\}, \tag{5}$$

and Gauss's law

$$\frac{\partial D_x}{\partial x}+\frac{\partial D_y}{\partial y}+\frac{\partial D_z}{\partial z}=0, \tag{6}$$

where c_{ij}, η_{kl}, and e_{kj} denote the elastic stiffness constant, dielectric constant, and piezoelectric constant, respectively [12]. The boundary conditions are then described as

$$\left.\begin{aligned}&x=0:\sigma_{zx}=-\tau_0 f(y,z),\sigma_{xx}=0,\sigma_{xy}=0,\Phi=0;\\&\sqrt{x^2+y^2+z^2}\to\infty:(u_x,u_y,u_z,\Phi)\to\mathbf{0}\end{aligned}\right\}. \tag{7}$$

2.3 Potential function method

According to the analytical technique previously proposed by us [12], the electroelastic field quantities are described by elastic displacement potential functions φ_i, piezoelastic displacement potential functions ϑ_i, certain constants k_i $(i=1,2)$, and electric potential Φ as follows:

$$\left.\begin{aligned} &u_x=\sum_{i=1}^{2}\left(\frac{\partial\varphi_i}{\partial x}+\frac{\partial\vartheta_i}{\partial y}\right),\quad u_y=\sum_{i=1}^{2}\left(\frac{\partial\varphi_i}{\partial y}-\frac{\partial\vartheta_i}{\partial x}\right),\\ &u_z=\frac{\partial}{\partial z}\sum_{i=1}^{2}k_i\varphi_i \end{aligned}\right\},\tag{8}$$

$$E_x=-\frac{\partial\Phi}{\partial x},\quad E_y=-\frac{\partial\Phi}{\partial y},\quad E_z=-\frac{\partial\Phi}{\partial z},\tag{9}$$

$$\left.\begin{aligned} &\varepsilon_{xx}=\sum_{i=1}^{2}\left(\frac{\partial^2\varphi_i}{\partial x^2}+\frac{\partial^2\vartheta_i}{\partial x\partial y}\right),\\ &\varepsilon_{yy}=\sum_{i=1}^{2}\left(\frac{\partial^2\varphi_i}{\partial y^2}-\frac{\partial^2\vartheta_i}{\partial x\partial y}\right),\ \varepsilon_{zz}=\sum_{i=1}^{2}k_i\frac{\partial^2\varphi_i}{\partial z^2},\\ &2\varepsilon_{yz}=\sum_{i=1}^{2}\left[(1+k_i)\frac{\partial^2\varphi_i}{\partial y\partial z}-\frac{\partial^2\vartheta_i}{\partial z\partial x}\right],\\ &2\varepsilon_{zx}=\sum_{i=1}^{2}\left[(1+k_i)\frac{\partial^2\varphi_i}{\partial z\partial x}+\frac{\partial^2\vartheta_i}{\partial y\partial z}\right],\\ &2\varepsilon_{xy}=\sum_{i=1}^{2}\left[2\frac{\partial^2\varphi_i}{\partial x\partial y}+\left(-\frac{\partial^2\vartheta_i}{\partial x^2}+\frac{\partial^2\vartheta_i}{\partial y^2}\right)\right] \end{aligned}\right\}.\tag{10}$$

The components of stress and electric displacement are obtained by a simple algebraic operation, namely by substituting equations (9) and (10) into equations (3) and (4). For the sake of brevity, only the components closely related to the boundary conditions and electroelastic coupling are shown as

$$\left.\begin{aligned} &\sigma_{xx}=\sum_{i=1}^{2}\left[\begin{aligned}&\left(c_{11}\frac{\partial^2\varphi_i}{\partial x^2}+c_{12}\frac{\partial^2\varphi_i}{\partial y^2}+k_ic_{13}\frac{\partial^2\varphi_i}{\partial z^2}\right)\\&+(c_{11}-c_{12})\frac{\partial^2\vartheta_i}{\partial x\partial y}\end{aligned}\right],\\ &\sigma_{xy}=\frac{c_{11}-c_{12}}{2}\sum_{i=1}^{2}\left[2\frac{\partial^2\varphi_i}{\partial x\partial y}+\left(-\frac{\partial^2\vartheta_i}{\partial x^2}+\frac{\partial^2\vartheta_i}{\partial y^2}\right)\right],\\ &\sigma_{yz}=c_{44}\sum_{i=1}^{2}\left[(1+k_i)\frac{\partial^2\varphi_i}{\partial y\partial z}-\frac{\partial^2\vartheta_i}{\partial z\partial x}\right]+e_{14}\frac{\partial\Phi}{\partial x},\\ &\sigma_{zx}=c_{44}\sum_{i=1}^{2}\left[(1+k_i)\frac{\partial^2\varphi_i}{\partial z\partial x}+\frac{\partial^2\vartheta_i}{\partial y\partial z}\right]-e_{14}\frac{\partial\Phi}{\partial y},\\ &D_x=e_{14}\sum_{i=1}^{2}\left[(1+k_i)\frac{\partial^2\varphi_i}{\partial y\partial z}-\frac{\partial^2\vartheta_i}{\partial z\partial x}\right]-\eta_{11}\frac{\partial\Phi}{\partial x},\\ &D_y=-e_{14}\sum_{i=1}^{2}\left[(1+k_i)\frac{\partial^2\varphi_i}{\partial z\partial x}+\frac{\partial^2\vartheta_i}{\partial y\partial z}\right]-\eta_{11}\frac{\partial\Phi}{\partial y} \end{aligned}\right\}.\tag{11}$$

The governing equations for φ_i, ϑ_i, and Φ are given by

$$\left.\begin{aligned} &\left(\frac{\partial^2}{\partial x^2}+\frac{\partial^2}{\partial y^2}+\mu_i\frac{\partial^2}{\partial z^2}\right)\varphi_i=0,\\ &\left(\frac{\partial^2}{\partial x^2}+\frac{\partial^2}{\partial y^2}+\upsilon_i\frac{\partial^2}{\partial z^2}\right)\vartheta_i=0,\\ &\frac{e_{14}}{c_{44}}\mu_3\frac{\partial\Phi}{\partial z}=\sum_{i=1}^{2}\left(\frac{\partial^2}{\partial x^2}+\frac{\partial^2}{\partial y^2}+\mu_3\frac{\partial^2}{\partial z^2}\right)\vartheta_i \end{aligned}\right\},\tag{12}$$

where μ_1 and μ_2 are the roots of a quadratic equation with respect to μ

$$c_{11}c_{44}\mu^2-\left(c_{11}c_{33}-c_{13}^2-2c_{13}c_{44}\right)\mu+c_{33}c_{44}=0,\tag{13}$$

υ_1 and υ_2 are the roots of a quadratic equation with respect to υ

$$\upsilon^2-\left[\mu_3\left(1+k_{\mathrm{couple}}^2\right)+\eta\right]\upsilon+\mu_3\eta=0;\tag{14}$$

$$\mu_3=\frac{2c_{44}}{c_{11}-c_{12}},\quad \eta=\frac{\eta_{33}}{\eta_{11}},\quad k_{\mathrm{couple}}^2=\frac{e_{14}^2}{c_{44}\eta_{11}},\tag{15}$$

and

$$k_i=\frac{c_{11}\mu_i-c_{44}}{c_{13}+c_{44}}=\frac{(c_{13}+c_{44})\mu_i}{c_{33}-c_{44}\mu_i}.\tag{16}$$

2.4 Formulae for electroelastic field quantities

As described in Subsection 2.1, the surface friction $\tau_0 f(y,z)$ is anti-symmetric and symmetric with respect to y and z, respectively, and so is the surface shear stress σ_{zx} obtained from equation (7). By referring to the fourth equation in equations (11), we find that φ_i is antisymmetric with respect to y and z, and that ϑ_i is symmetric and antisymmetric with respect to y and z, respectively. By considering these symmetric and anti-symmetric properties and the finiteness of the electroelastic field described by the second equation in equation (7), and applying the Fourier transform [13] to equation (12), the solutions for φ_i and ϑ_i $(i=1,2)$ are obtained as

$$\left.\begin{aligned} &\varphi_i=\int_0^\infty\int_0^\infty\left[\begin{aligned}&A_i(\alpha,\beta)\exp(-\gamma_{\mu i}x)\\&\cdot\sin(\alpha y)\sin(\beta z)\end{aligned}\right]\mathrm{d}\alpha\mathrm{d}\beta,\\ &\vartheta_i=\int_0^\infty\int_0^\infty\left[\begin{aligned}&C_i(\alpha,\beta)\exp(-\gamma_{\upsilon i}x)\\&\cdot\cos(\alpha y)\sin(\beta z)\end{aligned}\right]\mathrm{d}\alpha\mathrm{d}\beta\\ &\left(\gamma_{\mu i}=\left(\alpha^2+\mu_i\beta^2\right)^{1/2},\ \gamma_{\upsilon i}=\left(\alpha^2+\upsilon_i\beta^2\right)^{1/2}\right) \end{aligned}\right\},\tag{17}$$

which in turn give

$$\Phi=\frac{c_{44}}{e_{14}}\frac{1}{\mu_3}\cdot\sum_{i=1}^{2}\left\{\int_0^\infty\int_0^\infty\left[\begin{aligned}&(\mu_3-\upsilon_i)\beta C_i(\alpha,\beta)\exp(-\gamma_{\upsilon i}x)\\&\cdot\cos(\alpha y)\cos(\beta z)\end{aligned}\right]\mathrm{d}\alpha\mathrm{d}\beta\right\}\tag{18}$$

from the third equation in equation (12).

By substituting equations (17) and (18) into equations (8)-(11), the electroelastic field quantities are obtained. For the sake of brevity, only the components of equation (11) are shown as

$$\left.\begin{aligned}
\sigma_{xx} &= \frac{c_{44}}{\mu_3}\sum_{i=1}^{2}\int_0^\infty\int_0^\infty \left\{\begin{aligned}&\left[\begin{aligned}&\left(2\alpha^2+(1+k_i)\mu_3\beta^2\right)\\ &\quad\cdot A_i(\alpha,\beta)\exp(-\gamma_{\mu i}x)\\ &+2\gamma_{\upsilon i}\alpha C_i(\alpha,\beta)\exp(-\gamma_{\upsilon i}x)\end{aligned}\right]\\ &\cdot\sin(\alpha y)\sin(\beta z)\mathrm{d}\alpha\mathrm{d}\beta\end{aligned}\right\},\\
\sigma_{xy} &= \frac{c_{44}}{\mu_3}\sum_{i=1}^{2}\int_0^\infty\int_0^\infty \left\{\begin{aligned}&\left[\begin{aligned}&-2\gamma_{\mu i}\alpha A_i(\alpha,\beta)\exp(-\gamma_{\mu i}x)\\ &-\left(2\alpha^2+\upsilon_i\beta^2\right)\\ &\quad\cdot C_i(\alpha,\beta)\exp(-\gamma_{\upsilon i}x)\end{aligned}\right]\\ &\cdot\cos(\alpha y)\sin(\beta z)\mathrm{d}\alpha\mathrm{d}\beta\end{aligned}\right\},\\
\sigma_{yz} &= \frac{c_{44}}{\mu_3}\sum_{i=1}^{2}\int_0^\infty\int_0^\infty \left\{\begin{aligned}&\left[\begin{aligned}&\mu_3(1+k_i)\alpha\beta\\ &\quad\cdot A_i(\alpha,\beta)\exp(-\gamma_{\mu i}x)\\ &+\upsilon_i\gamma_{\upsilon i}\beta C_i(\alpha,\beta)\exp(-\gamma_{\upsilon i}x)\end{aligned}\right]\\ &\cdot\cos(\alpha y)\cos(\beta z)\mathrm{d}\alpha\mathrm{d}\beta\end{aligned}\right\},\\
\sigma_{zx} &= \frac{c_{44}}{\mu_3}\sum_{i=1}^{2}\int_0^\infty\int_0^\infty \left\{\begin{aligned}&\left[\begin{aligned}&-\mu_3(1+k_i)\gamma_{\mu i}\beta\\ &\quad\cdot A_i(\alpha,\beta)\exp(-\gamma_{\mu i}x)\\ &-\upsilon_i\alpha\beta C_i(\alpha,\beta)\exp(-\gamma_{\upsilon i}x)\end{aligned}\right]\\ &\cdot\sin(\alpha y)\cos(\beta z)\mathrm{d}\alpha\mathrm{d}\beta\end{aligned}\right\},\\
D_x &= \frac{c_{44}\eta_{11}}{e_{14}\mu_3}\sum_{i=1}^{2}\int_0^\infty\int_0^\infty \left\{\begin{aligned}&\left[\begin{aligned}&\mu_3k_{\mathrm{couple}}^2(1+k_i)\alpha\beta\\ &\quad\cdot A_i(\alpha,\beta)\exp(-\gamma_{\mu i}x)\\ &+\left(\mu_3\left(1+k_{\mathrm{couple}}^2\right)-\upsilon_i\right)\gamma_{\upsilon i}\beta\\ &\quad\cdot C_i(\alpha,\beta)\exp(-\gamma_{\upsilon i}x)\end{aligned}\right]\\ &\cdot\cos(\alpha y)\cos(\beta z)\mathrm{d}\alpha\mathrm{d}\beta\end{aligned}\right\},\\
D_y &= \frac{c_{44}\eta_{11}}{e_{14}\mu_3}\sum_{i=1}^{2}\int_0^\infty\int_0^\infty \left\{\begin{aligned}&\left[\begin{aligned}&\mu_3k_{\mathrm{couple}}^2(1+k_i)\gamma_{\mu i}\beta\\ &\quad\cdot A_i(\alpha,\beta)\exp(-\gamma_{\mu i}x)\\ &+\left(\mu_3\left(1+k_{\mathrm{couple}}^2\right)-\upsilon_i\right)\alpha\beta\\ &\quad\cdot C_i(\alpha,\beta)\exp(-\gamma_{\upsilon i}x)\end{aligned}\right]\\ &\cdot\sin(\alpha y)\cos(\beta z)\mathrm{d}\alpha\mathrm{d}\beta\end{aligned}\right\}
\end{aligned}\right\}. \quad \text{... (19)}$$

The distribution function for surface friction, $f(y,z)$, is expressed in Fourier integral form [13] as

$$f(y,z)=\int_0^\infty\int_0^\infty f^*(\alpha,\beta)\sin(\alpha y)\cos(\beta z)\mathrm{d}\alpha\mathrm{d}\beta, \quad (20)$$

where

$$f^*(\alpha,\beta)=\frac{4}{\pi^2}\int_0^\infty\int_0^\infty f(y,z)\sin(\alpha y)\cos(\beta z)\mathrm{d}y\mathrm{d}z\,. \quad (21)$$

By substituting equations (18)-(20) into equation (7), a set of simultaneous equations for $A_i(\alpha,\beta)$ and $C_i(\alpha,\beta)$ $(i=1,2)$ is obtained as

$$\left.\begin{aligned}
&\sum_{i=1}^{2}\left[\begin{aligned}&\left(2\alpha^2+(1+k_i)\mu_3\beta^2\right)A_i(\alpha,\beta)\\ &+2\gamma_{\upsilon i}\alpha C_i(\alpha,\beta)\end{aligned}\right]=0,\\
&\sum_{i=1}^{2}\left[\mu_3(1+k_i)\gamma_{\mu i}A_i(\alpha,\beta)+\upsilon_i\alpha C_i(\alpha,\beta)\right]\\
&\quad=\frac{\mu_3\tau_0}{c_{44}}\frac{f^*(\alpha,\beta)}{\beta},\\
&\sum_{i=1}^{2}\left[-2\gamma_{\mu i}\alpha A_i(\alpha,\beta)-\left(2\alpha^2+\upsilon_i\beta^2\right)C_i(\alpha,\beta)\right]=0,\\
&\sum_{i=1}^{2}(\mu_3-\upsilon_i)C_i(\alpha,\beta)=0
\end{aligned}\right\}. \quad (22)$$

The solution to this is obtained as

$$\begin{Bmatrix}A_1(\alpha,\beta)\\A_2(\alpha,\beta)\\C_1(\alpha,\beta)\\C_2(\alpha,\beta)\end{Bmatrix}=\frac{\tau_0}{c_{44}}\frac{f^*(\alpha,\beta)}{\beta}\frac{1}{\Delta(\alpha,\beta)}\begin{Bmatrix}A_1^*(\alpha,\beta)\\A_2^*(\alpha,\beta)\\C_1^*(\alpha,\beta)\\C_2^*(\alpha,\beta)\end{Bmatrix} \quad (23)$$

together with

$$\left.\begin{aligned}
&\Delta(\alpha,\beta)\\
&\equiv 2\left[2\mu_3-(\upsilon_1+\upsilon_2)\right](k_1-k_2)\alpha^2\gamma_{\mu1}\gamma_{\mu2}(\gamma_{\upsilon1}-\gamma_{\upsilon2})\\
&\quad+(\upsilon_1-\upsilon_2)\left\{\begin{aligned}&2(k_1-k_2)\alpha^2\\ &\quad\cdot\left[\gamma_{\mu1}\gamma_{\mu2}(\gamma_{\upsilon1}+\gamma_{\upsilon2})-\mu_3\beta^2(\gamma_{\mu1}+\gamma_{\mu2})\right]\\ &-\mu_3(1+k_1)(1+k_2)\\ &\quad\cdot\left(2\alpha^2+\mu_3\beta^2\right)\beta^2(\gamma_{\mu1}-\gamma_{\mu2})\\ &-4\alpha^4(k_1\gamma_{\mu1}-k_2\gamma_{\mu2})\end{aligned}\right\},\\
&A_1^*(\alpha,\beta)\\
&\equiv-(\upsilon_1-\upsilon_2)\left[2\alpha^2+(1+k_2)\mu_3\beta^2\right]\left(2\alpha^2+\mu_3\beta^2\right)\\
&\quad+4\gamma_{\mu2}\alpha^2\left[\mu_3(\gamma_{\upsilon1}-\gamma_{\upsilon2})+\upsilon_1\gamma_{\upsilon2}-\upsilon_2\gamma_{\upsilon1}\right],\\
&A_2^*(\alpha,\beta)\\
&\equiv+(\upsilon_1-\upsilon_2)\left[2\alpha^2+(1+k_1)\mu_3\beta^2\right]\left(2\alpha^2+\mu_3\beta^2\right)\\
&\quad-4\gamma_{\mu1}\alpha^2\left[\mu_3(\gamma_{\upsilon1}-\gamma_{\upsilon2})+\upsilon_1\gamma_{\upsilon2}-\upsilon_2\gamma_{\upsilon1}\right],\\
&C_1^*(\alpha,\beta)\equiv2(\mu_3-\upsilon_2)\alpha\\
&\quad\cdot\left\{\begin{aligned}&2(\gamma_{\mu1}-\gamma_{\mu2})\alpha^2\\ &+\mu_3\beta^2\left[(\gamma_{\mu1}-\gamma_{\mu2})-(k_1\gamma_{\mu2}-k_2\gamma_{\mu1})\right]\end{aligned}\right\},\\
&C_2^*(\alpha,\beta)\equiv-2(\mu_3-\upsilon_1)\alpha\\
&\quad\cdot\left\{\begin{aligned}&2(\gamma_{\mu1}-\gamma_{\mu2})\alpha^2\\ &+\mu_3\beta^2\left[(\gamma_{\mu1}-\gamma_{\mu2})-(k_1\gamma_{\mu2}-k_2\gamma_{\mu1})\right]\end{aligned}\right\}
\end{aligned}\right\}. \quad \text{... (24)}$$

By substituting equations (23) and (24) into equation (19), the electroelastic field quantities are formulated. Thus, our purpose in this section has been attained. Although for a simple model, these formulae are advantageous in that they enable us to evaluate field quantities without errors, and to investigate quantities *inside* the body, namely experimentally-unmeasurable quantities.

III. Numerical calculation

3.1 Numerical specifications

The distribution function for surface friction, $f(y,z)$, is assumed to have a Rayleigh distribution with respect to y and a Gaussian distribution with respect to z, with an effective width δ as

$$f(y,z)=\frac{y}{\delta}\exp\left(-\frac{y^2}{\delta^2}\right)\cdot\exp\left(-\frac{z^2}{\delta^2}\right), \qquad (25)$$

for which equation (21) is calculated as

$$f^*(\alpha,\beta)=\frac{\alpha\delta^3}{2\pi}\exp\left[-\frac{(\alpha\delta)^2+(\beta\delta)^2}{4}\right]. \qquad (26)$$

It should be noted that $f(y,z)$ in Fig. 1 is shown actually as defined by equation (25).

As an example of a piezoelectric body, we chose Sitka spruce (*Picea sitchensis*). Although a complete set of its material constants was not found in a common condition or in the form of equations (3) and (4), it was built in our past work [12] as

$$\left.\begin{aligned}
&c_{11}=830.84[\mathrm{MPa}],\ c_{33}=12.276[\mathrm{GPa}],\\
&c_{12}=294.47[\mathrm{MPa}],\ c_{13}=472.07[\mathrm{MPa}],\\
&c_{44}=742.50[\mathrm{MPa}],\\
&\eta_{11}=16.823\times10^{-12}\left[\mathrm{C^2N^{-1}m^{-2}}\right],\\
&\eta_{33}=22.490\times10^{-12}\left[\mathrm{C^2N^{-1}m^{-2}}\right],\\
&e_{14}=-0.14850\times10^{-3}\left[\mathrm{Cm^{-2}}\right]
\end{aligned}\right\}. \qquad (27)$$

To show the numerical results, we introduced the following nondimensional quantities:

$$\left.\begin{aligned}
&(\hat{x},\hat{y},\hat{z})\equiv\frac{(x,y,z)}{\delta},\\
&(\hat{c}_{11},\hat{c}_{12},\hat{c}_{13},\hat{c}_{33})\equiv\frac{(c_{11},c_{12},c_{13},c_{33})}{c_{44}},\\
&(\hat{\sigma}_{yz},\hat{\sigma}_{zx})\equiv\frac{(\sigma_{yz},\sigma_{zx})}{\tau_0},\ (\hat{D}_x,\hat{D}_y)\equiv\frac{(D_x,D_y)}{\left(\dfrac{|e_{14}|\tau_0}{c_{44}}\right)}
\end{aligned}\right\}. \qquad (28)$$

For brevity, we hereafter omit the signs for nondimensional quantities, $\frown$.

3.2 Distributions of field quantities

Figure 2, which is expressed by equation (19), shows the distribution of stress σ_{zx} inside the body. From Fig. 2, we see that stress σ_{zx} is maximum at the surface $x=0$ and decreases monotonically toward zero with x to satisfy the finiteness of the field described by equation (7). Figure 2 shows one of the most important aspects of this study: electroelastic field quantities *inside* the body, which are nearly impossible to obtain experimentally, are obtained.

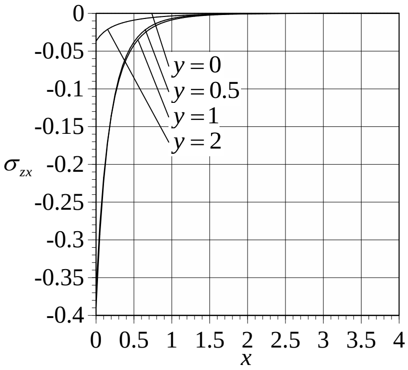

Fig. 2: Distribution of stress σ_{zx} inside the body $(z=0)$

Figures 3 and 4 show the distributions of stress σ_{zx} and σ_{yz}, respectively, on the surface $x=0$. It should be noted that the direction of the y-axis was taken as in the left part of Fig. 1. By referring to Fig. 1, which shows the distribution of $f(y,z)$ as defined by equation (25), we found that the numerical results in Fig. 3 satisfied the boundary condition described by the first equation in equations (7), namely $(\sigma_{zx})_{x=0}=-f(y,z)$. From Fig. 4, we found that stress σ_{yz}, for respective values of z, was positive and maximum at $y=0$, decreased to a negative and minimum value with y, and finally converged to zero for $y\to\infty$ to satisfy the finiteness of the field described by equation (7).

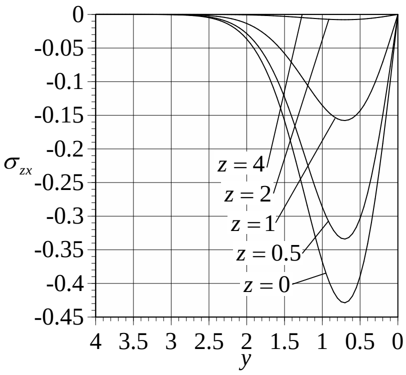

Fig. 3: Distribution of stress σ_{zx} on the surface $x=0$

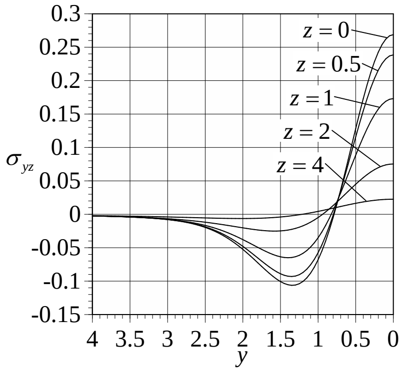

Fig. 4: Distribution of stress σ_{yz} on the surface $x=0$

Figures 5 and 6 show that the magnitudes of electric displacements D_x and D_y were maximum at the surface $x=0$, and decreased to zero with x. Figures 5 and 6 also show the important aspect mentioned with regard to Fig. 2 above because both figures elucidate experimentally-unmeasurable quantities.

At the same time, experimentally-measurable responses to disturbances need to be investigated from the viewpoint of nondestructive evaluation techniques. By regarding surface friction $f(y,z)$ in Fig. 1 as such a disturbance, the electric displacement D_x on the surface $x=0$ is one of the candidates for such a response. From this viewpoint, the distribution of electric displacement D_x on the surface $x=0$ is shown in Fig. 7, where the direction of the y-axis was taken as that in Fig. 4. By comparing Fig. 7 with Fig. 4, we found that the variations in electric displacement D_x with y for various values of z were roughly proportional to those of stress σ_{yz}. This tendency was considered to be a consequence of the coupling behavior in σ_{yz}, ε_{yz}, D_x, and E_x through the piezoelectric constant e_{14} in the fourth and first lines of equations (3) and (4), respectively, and suggested the possibility of a nondestructive evaluation technique using piezoelectric signals. Although the electroelastic response discussed in this paper occurred due to the disturbance defined in equation (25), responses for other disturbances can be easily investigated by updating $f(y,z)$ in equation (21). Furthermore, we expect that various configurations of the body, including bodies with defects such as notches, cracks, or inclusions, can be analyzed because the governing equations (12) for φ_i and ϑ_i are essentially the Laplace equations, which are mathematically well established.

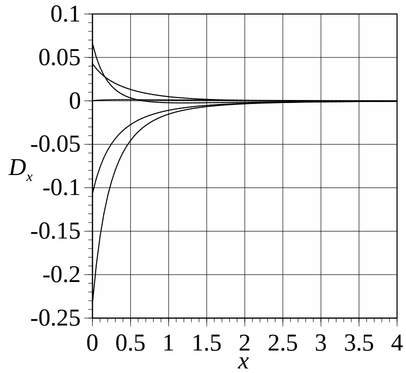

Fig. 5: Distribution of electric displacement D_x inside the body $(z=0)$

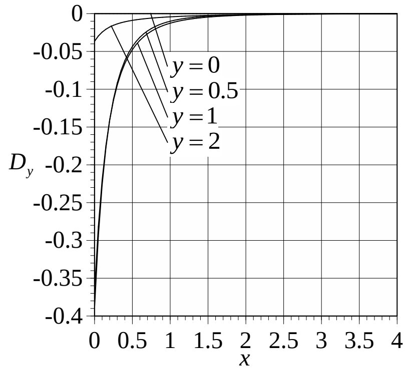

Fig. 6: Distribution of electric displacement D_y inside the body $(z=0)$

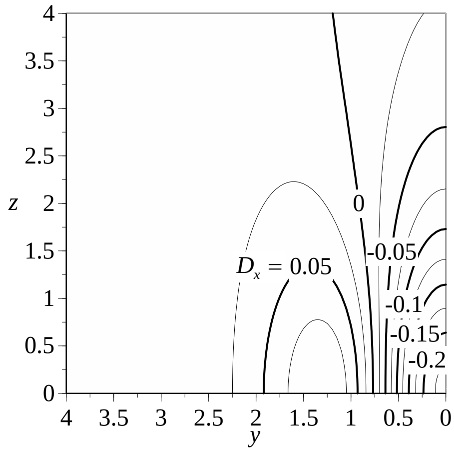

Fig. 7: Distribution of electric displacement D_x on the surface $x=0$

IV. Concluding remarks

In this paper, we studied the electroelastic field in a semi-infinite body with D_∞ symmetry subjected to surface friction. We theoretically formulated electroelastic field quantities by the potential function method and obtained the distributions of electroelastic field quantities inside the body by numerical calculations. These achievements, although their success depends on the characteristics of the model, have a great significance because they enable us to accurately evaluate actual field quantities and to investigate experimentally-unmeasurable quantities.

Moreover, we quantitatively investigated the surface electric displacement in response to an elastic stimulus of the surface friction and suggested the possibility of a nondestructive evaluation technique using piezoelectric signals.

References

[1] E. Fukada, Piezoelectricity of wood, *Journal of the Physical Society of Japan, 10(2)*, 1955, 149-154.

[2] J.A. Smetana and P.W. Kelso, Piezoelectric charge density measurements on the surface of Douglas-fir, *Wood Science, 3(3)*, 1971, 161-171.

[3] W. Knuffel and A. Pizzi, The piezoelectric effect in structural timber, *Holzforschung, 40(3)*, 1986, 157-162.

[4] W.E. Knuffel, The piezoelectric effect in structural timber - part II. The influence of natural defects, *Holzforschung, 42(4)*, 1988, 247-252.

[5] T. Nakai, N. Igushi, and K. Ando, Piezoelectric behavior of wood under combined compression and vibration stresses I: Relation between piezoelectric voltage and microscopic deformation of a Sitka spruce (Picea sitchensis Carr.), *Journal of Wood Science, 44(1),* 1998, 28-34.

[6] T. Nakai and K. Ando, Piezoelectric behavior of wood under combined compression and vibration stresses II: Effect of the deformation of cross-sectional wall of tracheids on changes in piezoelectric voltage in linear-elastic region, *Journal of Wood Science, 44(4)*, 1998, 255-259.

[7] T. Nakai, M. Hamatake, and T. Nakao, Relationship between piezoelectric behavior and the stress – strain curve of wood under combined compression and vibration stresses, *Journal of Wood Science, 50(1),* 2004, 97-99.

[8] T. Nakai, H. Yamamoto, M. Hamatake, and T. Nakao, Initial shapes of stress-strain curve of wood specimen subjected to repeated combined compression and vibration stresses and the piezoelectric behavior, *Journal of Wood Science, 52(6)*, 2006, 539-543.

[9] N. Hirai, I. Asano, and N. Sobue, Piezoelectric anisotropy of wood, *Journal of the Society of Materials Science, Japan, 22(241)*, 1973, 948-955 (in Japanese).

[10] N. Hirai, N. Sobue, and M. Date, New piezoelectric moduli of wood: d31 and d32, *Journal of Wood Science, 57(1)*, 2011, 1-6.

[11] S.K. Kim, *Group theoretical methods and applications to molecules and crystals* (Cambridge: Cambridge University Press, 1999).

[12] M. Ishihara, Y. Ootao, and Y. Kameo, Analytical technique for electroelastic field in piezoelectric bodies belonging to point broup D_∞, *Journal of Wood Science, 61(3)*, 2015, 270-284.

[13] I.N. Sneddon, *The use of integral transforms* (New York: McGraw-Hill, 1972).